Investigating Protein−Ligand Interactions with a Mutant FKBP Possessing a Designed Specificity Pocket

Wu Yang, Leonard W. Rozamus, Surinder Narula, Carl T. Rollins, Ruth Yuan, Lawrence J. Andrade, Mary K. Ram, Thomas B. Phillips, Marie Rose van Schravendijk, David Dalgarno, Tim Clackson,* and Dennis A. Holt*

ARIAD Gene Therapeutics, 26 Landsdowne Street, Cambridge, Massachusetts 02139-4234

Received August 25, 1999

Using structure-based design and protein mutagenesis we have remodeled the FKBP12 ligand binding site to include a sizable, hydrophobic specificity pocket. This mutant (F36V-FKBP) is capable of binding, with low or subnanomolar affinities, novel synthetic ligands possessing designed substituents that sterically prevent binding to the wild-type protein. Using binding and structural analysis of bumped compounds, we show here that the pocket is highly promiscuous—capable of binding a range of hydrophobic alkyl and aryl moieties with comparable affinity. Ligand affinity therefore appears largely insensitive to the degree of occupancy or quality of packing of the pocket. NMR spectroscopic analysis indicates that similar ligands can adopt radically different binding modes, thus complicating the interpretation of structure−activity relationships.

Introduction

Traditionally, our understanding of how small molecules bind protein targets has come from structure−activity relationships, derived from the binding of series of iteratively modified compounds to a single protein. These studies have revealed the importance of features such as shape complementarity, hydrogen bonding, and ligand preordering.[1] More recently, the ability to specifically mutate proteins using recombinant DNA technology has allowed an extension of this approach: both the protein target and its small molecule ligand can be modified, for example, to insert a cavity into the ligand binding site and design a complementary ligand "bump".[2−10] Analysis of such remodeled complexes might provide new insights into the factors important to binding affinity and specificity and may also guide attempts to design drugs for naturally "mutated" proteins, such as homologous family members[11,12] or protein targets that mutate during the evolution of microbial drug resistance.

We have been remodeling the high-affinity interface between FKBP12 and relatively simple ligands to develop improved chemical inducers of dimerization (CIDs)[13] for directing protein−protein association inside cells. Bivalent dimers of wholly synthetic ligands which are capable of simultaneously binding two FKBP molecules, and thus able to dimerize or oligomerize chimeric proteins containing FKBP domains, have been used to control signal transduction and gene expression events in genetically engineered cells.[14−16] Because these compounds bind equally well to endogenous FKBP12 and to their intended FKBP-fusion targets, they hypothetically could interfere with the normal physiological functions of FKBP. In addition, these compounds might suffer reduced potency due to sequestration by the ubiquitous wild-type protein. To overcome these potential limitations, we designed new ligands which have greatly reduced affinity for wild-type FKBP12, but which possess high affinity for minimally mutated FKBP domains of the chimeric receptor proteins.[9]

The process of metamorphosing both target protein and ligand to achieve a novel pattern of selectivity began with the aid of structural modeling. These studies suggested that pyramidalization and appropriate substitution of C9 of a typical pipecolyl α-ketoamide ligand (e.g., **1**[17]) would introduce a sterically encumbering "bump" that would prevent binding to wild-type FKBP, but which might be accommodated by a compensatory "hole" created in the protein by a single mutation of Phe36 to a smaller hydrophobic amino acid (Figure 1).[10] Indeed, compound **2S** was shown to have exceptional affinity for F36V-FKBP with a K_d of ca. 100 pM while having negligible affinity for wild-type FKBP12.[9] Subsequent structure determination of the F36V-FKBP/**2S** complex by X-ray crystallography confirmed the predicted binding mode, showing that the C9 ethyl substituent (the bump) partially, but not completely, fills the 90 Å^3 hole created by the F36V mutation (Figure 2).[9]

In this study we set out to probe molecular recognition in this engineered binding site by determining the specificity of the F36V hole for various bumps. We prepared a series of α-substituted trimethoxyphenylacetamide and phenylacetamide derivatives with bumps ranging in size from hydrogen (no bump) to cyclohexyl and analyzed their binding to F36V-FKBP by using a combination of affinity measurements and NMR structural studies.

Results and Discussion

Trimethoxyphenylacetamide Series. We first examined binding of the trimethoxyphenylacetamide series to the mutated protein. Initial molecular modeling

* To whom correspondence should be addressed. Phone: 617-494-0400. Fax: 617-225-2589. E-mail: holtd@tiac.net, clackson@ariad.com.

10.1021/jm9904396 CCC: $19.00
Published on Web 02/25/2000

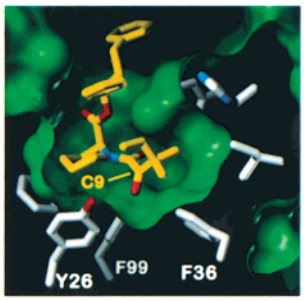

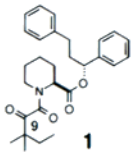

Figure 1. X-ray crystal structure of **1** bound to FKBP12.[17] A cut-away view of the calculated solvent accessible surface of the protein in the ligand binding region is shown in green.

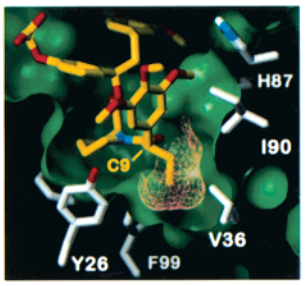

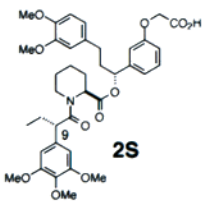

Figure 2. X-ray crystal structure of **2S** bound to F36V-FKBP.[9] Portions of the calculated solvent accessible surfaces of the protein and ligand are shown as solid green surface and orange mesh, respectively.

studies suggested that C9 alkyl substituents in the *S* configuration would more optimally engage the hole created by the F36V mutation than those of the *R* configuration. This expectation was born out as **2S** exhibits a 100-fold higher affinity than its C9-epimeric analogue (**2R**, Table 1).[9] That compound **2R** retains reasonable affinity for F36V-FKBP, while having no detectable affinity for the wild-type protein, suggests that the *R*-configured ethyl bump is still accommodated by the engineered protein hole, albeit at an energetic cost of nearly 3 kcal/mol. NMR structure determinations of the **2S** and **2R** complexes with F36V-FKBP revealed similar ligand conformations relative to each other (Figure 3, **2S** and **2R**) and to that observed previously[9] in the crystal structure of **2S** (Figure 2). The pipecolyl and trimethoxyphenyl rings of **2R** and **2S** are nearly superimposable. The latter occupies a natural pocket—defined by residues Asp37, His87, and Ile90—which also binds the tetrahydropyranyl (THP) moiety of FK506 and rapamycin. Whereas the ethyl group of **2S** has the most direct approach into the F36V hole, Figure 3 illustrates that the C9 ethyl substituent of **2R** is also able to engage the hole. Presumably, reduced contact of the *R*-ethyl group with the hydrophobic hole and/or a degree of steric repulsion with Tyr26 leads to the reduced affinity of **2R** relative to **2S**.

Recognizing that some 50−60 Å^3 of the F36V hole remains unoccupied while coordinated with **2S**, a series of analogues with progressively larger bumps was prepared in an attempt to enhance affinity by more completely filling the engineered hole. In fact, the binding of the *S*-trimethoxyphenyl analogues appears to be remarkably insensitive to modest changes to the bump (Table 1). The corresponding *R* analogues show somewhat greater enhancements to binding with increasing bump size. The *R*-allyl compound (**3R**) exhibits the highest affinity of the subset having 10-fold higher affinity than the *R*-ethyl compound (**2R**). In keeping with the original model of binding, for each diastereomeric pair the *S* analogue is preferred, implying that the overall binding mode of **3**−**6** is the same as **2**.

Phenylacetamide Series. Previously, we showed that C9 bump moieties could be combined with several suitable "bottom" groups in place of trimethoxyphenyl. The phenyl for trimethoxyphenyl substitution results in a loss of affinity (20-fold for **2S** vs **9S**), but specificity is retained.[9] Therefore, we also examined the specificity of bump moieties to F36V-FKBP in the more readily prepared phenyl congeneric series. In the *S* series, the ethyl analogue (**9S**) exhibits the highest affinity for F36V-FKBP (Table 2). The affinity of the methyl analogue (**8S**) is reduced approximately 2-fold which is still some 15-fold better than the unsubstituted (unbumped) analogue (**7**). Incorporation of isopropyl as the bump (**10S**) results in a 4-fold loss in affinity relative to the ethyl (**9S**), similar to the difference observed between **2S** and **5S**, possibly owing to unfavorable steric interactions of the branched isopropyl side chain at the mouth of the F36V hole. Model building suggests that the engineered hole is capable of accommodating a cyclohexyl substituent with only minimal distortion of the protein. Although similar steric clashes are likely to occur for cyclohexyl as for isopropyl, the additional hydrophobic interactions available to the cyclohexyl presumably accounts for a 2-fold binding advantage relative to the isopropyl analogue and restores the affinity of **11S** to within 1.5-fold of the ethyl analogue (**9S**). As observed for the *S* series of trimethoxyphenyl congeners, the affinities of the phenyl analogues are largely independent of the size of the bump. Only a 4-fold range of IC_{50}s is seen in the methyl to cyclohexyl series. At the extreme, incorporation of phenyl as the bump (**12**) results in only a 7-fold reduction in affinity in comparison to **9S**.

Examination of the *R*-congeneric series reveals a remarkably different structure−activity trend. Whereas the *R*-methyl analogue (**8R**) and *R*-ethyl analogue (**9R**) are both less active than their *S*-configured analogues (**8S** and **9S**)—as the original bump-hole design had predicted—a reversal in the stereochemical preference is seen for the *R*-isopropyl and *R*-cyclohexyl analogues. Both **10R** and **11R** exhibit roughly 6-fold higher affinity than their corresponding *S* analogues. The explanation for this reversal is apparent from the NMR structures

Table 1. Trimethoxyphenylacetamide Series: Binding Affinities (IC_{50}s, nM) for F36V-FKBP

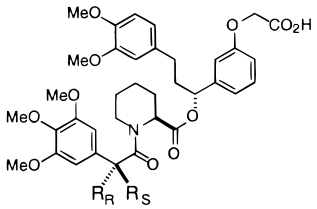

compd no.	bump	*R* series R_S = H R_R = bump	*S* series R_S = bump R_R = H
2 (R,S)	Et	187	1.8
3 (R,S)	allyl	19	1.5
4 (R,S)	*n*-Pr	43	3.8
5 (R,S)	*i*-Pr	65	5.8
6 (R,S)	c-PrCH$_2$	126	4.4

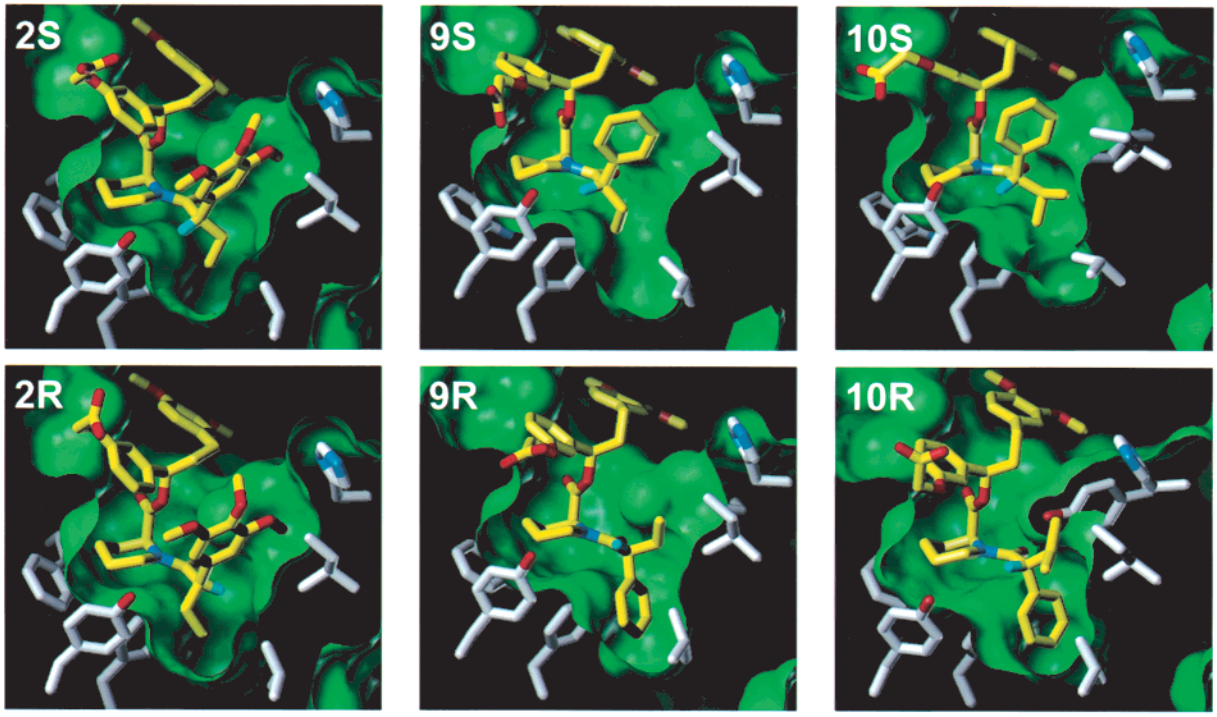

Figure 3. NMR-derived structural models of **2S**, **2R**, **9S**, **9R**, **10S**, and **10R** bound to F36V-FKBP. Carbon atoms of the ligands are shown in yellow; C9 hydrogen atoms are shown in cyan. Portions of the calculated solvent accessible surfaces are shown as solid green surfaces.

Table 2. Phenylacetamide Series: Binding Affinities (IC_{50}s, nM) for F36V-FKBP

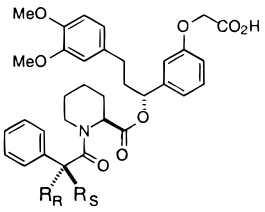

compd no.	bump	*R* series R_S = H R_R = bump	*S* series R_S = bump R_R = H
7	H	1530	
8 (R,S)	Me	590	94
9 (R,S)	Et	133	40
10 (R,S)	*i*-Pr	19	150
11 (R,S)	c-Hx	12	66
12	Ph	273	

of ethyl analogues **9R** and **9S** and isopropyl analogues **10R** and **10S** (Figure 3). The *R* series bind in a nearly identical fashion as the *S* series with the exception of a 120° torsional rotation about the C8−C9 bond. For the *R* compounds this leads to a positioning of the *phenyl* C9 substituent into the F36V engineered hole and allows the variable bump substituent to take station in the now-vacated THP-binding pocket. Thus, despite the apparent inconsistency in SAR, the *R*- and *S*-phenylacetamide derivatives adopt a common orientation where the C9 proton is always pointing toward Phe99. That **2R**, and presumably other *R*-trimethoxyphenylacetamide analogues, adopts a different binding mode—one where the C9 hydrogen is pointed toward Val36 (Figure 3)—suggests that the trimethoxyphenyl moiety is too large to enter the engineered hole and remains fixed in the THP-binding pocket. The divergent SAR for the *R* series of phenylacetamide analogues (**8**−**11**) reflects the different propensities for the alkyl groups

Scheme 1

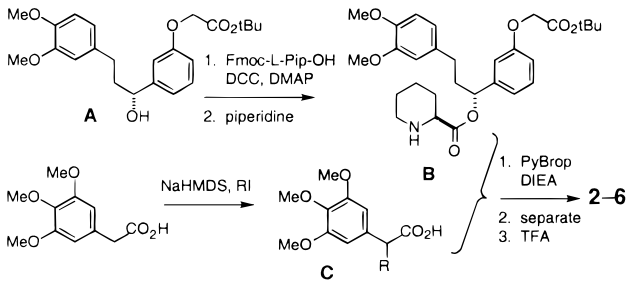

(methyl < ethyl < isopropyl ≈ cyclohexyl) to bind in the larger THP-binding pocket while the phenyl group is engaging the engineered hole. This SAR trend for alkyl groups occupying the THP-binding pocket is identical to that reported for simple, unbumped FKBP12 ligands.[18] The affinity of the C9-symmetrical diphenyl analogue (**12**) for F36V-FKBP suggests that the THP-binding pocket prefers occupation by the branched alkyls, isopropyl and cyclohexyl, over phenyl by some 15- to 20-fold (**12** vs **10R** and **11R**), whereas the engineered F36V hole has a lower preference for those same branched alkyls over phenyl by a factor of only 2- to 4-fold (**12** vs **10S** and **11S**). Thus, in comparing **10R** vs **10S** or **11R** vs **11S**, F36V-FKBP preferentially binds the *R* analogues in order to place the alkyl groups in the THP-binding pocket and the phenyl moiety in the engineered hole.

Synthesis. The pipecolyl trimethoxyphenylacetamides of Table 1 were prepared by conventional means as illustrated in Scheme 1. Enantiomerically pure diarylpropanol **A** was previously described. Following coupling of **B** and **C**, diastereomers were separated chromatographically prior to final *tert*-butyl ester deprotection. The analogous phenylacetamides of Table 2 were prepared similarly.

Conclusions

At the extremes of classic protein−ligand recognition paradigms are the lock-and-key and induced-fit models. In each case, whether the protein is assumed to be quite rigid as in the former or to have greater plasticity as in the latter, a highly complementary packing of protein and ligand has been thought to be characteristic of high-affinity interactions. In this and a preceding study we have shown that such precision in fit is not required, at least for the hydrophobic interface we studied. In this example, a single F36V mutation in FKBP12 opens a cavity of approximately 90 Å^3 at the base of the natural binding site. This engineered hole, designed as a specificity pocket, is remarkably stable and retains its shape even when unoccupied (as shown by a crystal structure of the protein bound to FK506[19]). While the binding of ligands possessing specificity elements (bumps) relies on the presence of this hole, complete filling of the hole by the bump is not required for high-affinity interactions. As a consequence, this specificity pocket appears to be surprisingly promiscuous in the accommodation of nonpolar ligand motifs ranging in size from methyl to cyclohexyl.

Despite examples to the contrary,[20] a nearly unavoidable assumption in the interpretation of structure−activity relationships is that common ligand cores result in common binding modes. Here, we studied ligand binding preferences of two pockets within a binding site—one natural (THP) and the other an engineered cavity. Unexpectedly, we found that the binding mode of compounds can "flip", positioning the moiety targeted for the engineered cavity in the THP-binding pocket and vice versa. This observation underscores the need for caution and the utility of spectroscopic verification in protein-binding structure−activity studies of congeneric small molecules.

Although F36V-FKBP is the first remodeled protein−small molecule interface to be structurally elucidated, promiscuous recognition and a toleration of imperfectly packed nonpolar interactions may prove to be general features of such interfaces.[10] Models of novel pairings between cyclophilin and cyclosporin[7,8,21] and between tyrosine kinases and ATP[2−6] generally indicate that unfilled cavities would remain after ligand binding, unless protein structural adjustments occurred.[10] One study of "bumped" pyrazolo[3,4-*d*]pyrimidine analogues binding to mutated tyrosine kinases found a variety of nonpolar cyclic substituents were tolerated in the engineered hole with similar affinities, albeit in the micromolar range.[6] Structural studies similar to those described here will be required to determine whether this behavior involves protein adjustments or changes in binding mode. Nevertheless, at least for the hydrophobic cavities engineered to date, it is clear that tightly packed complementarity is not a prerequisite for high-affinity binding.

Reengineered (orthogonal) protein−small molecule pairs are potentially powerful tools for a variety of biological problems because they allow an otherwise nonspecific small molecule to be restricted to a single (engineered) target protein inside cells.[10] Thus, the consequences of an inhibition,[3,6,8] activation,[9,22] or enzyme turnover event[2,5,23] can be studied and/or controlled in isolation. For example, chemical dimerizers built from the FKBP ligands described here may be more efficient at activating transcription or signal transduction events, by virtue of their specific interaction with target FKBP fusion proteins and not endogenous FKBP.[9,15,16] Our results provide guidance for the reengineering of other binding partners for dissecting and controlling complex biological pathways. In addition, proteins with binding sites containing engineered cavities can be thought of as model systems for natural protein drug targets that closely resemble other, nontarget proteins (such as homologues within a protein family[11,12]). Our results imply that specific, high-affinity ligands for such natural variants may be more easily obtained than was previously appreciated.

Experimental Section

(1*R*)-3-(3,4-Dimethoxyphenyl)-1-[3-(*t*-butoxycarbonylmethoxy)phenyl]-1-propyl (2*S*)-1-(9-Fluorenylmethoxycarbonyl)-2-piperidinecarboxylate. A solution of (*R*)-1-(3-(*t*-butoxycarbonylmethoxy)phenyl)-3-(3,4-dimethoxyphenyl) propan-1-ol[15,16] (**A**, 3.1 g, 7.7 mmol) in CH_2Cl_2 (40 mL) was treated with *N*-Fmoc-L-pipecolic acid (3.0 g, 8.5 mmol) followed by 1,3-dicyclohexyl carbodiimide (DCC, 1.9 g, 9.2 mmol) and 4-(dimethylamino)pyridine (DMAP, 560 mg, 4.6 mmol) under a nitrogen atmosphere. The resulting white suspension was allowed to stir overnight at ambient temperature. The reaction mixture was then filtered, evaporated, and flash chromatographed (silica gel, 15 to 20% EtOAc/hexanes) to afford 4.7 g (83%) of the Fmoc-protected pipecolyl ester as a white foam: IR (neat) 2939, 1746, 1702, 1516, 1451, 1258, 1154, 760, 740 cm^{-1}; ^{1}H NMR ($CDCl_3$, 300 MHz) 7.73 (m, 2H), 7.59 (t, J = 6.6 Hz, 1H), 7.16−7.49 (m, 6H), 6.94 (d, J = 7.6 Hz, 1H), 6.89 (s, 1H), 6.72−6.82 (m, 2H), 6.62 (m, 2H), 5.76 (br s, 1H), 5.02 (d, J = 3.7 Hz, 1H), 4.25−4.49 (m, 5H), 4.07−4.14 (m, 1H), 3.83 (s, 6H), 3.14 (t, J = 11.1 Hz, 1H), 2.46−2.54 (m, 2H), 2.16−2.33 (m, 2H), 2.00−2.07 (m, 1H), 1.68−1.78 (m, 4H), 1.46 (s, 9H), 1.39−1.56 (m, 1H); ^{13}C NMR ($CDCl_3$, 75 MHz) 174.50, 171.33, 168.28, 158.48, 147.73, 144.30, 142.12, 133.90, 130.07, 128.07, 127.45, 125.48, 120.50, 120.35, 114.34, 113.66, 112.12, 111.74, 82.74, 76.82, 76.59, 68.20, 66.16, 56.32, 56.20, 47.63, 38.44, 31.98, 31.54, 28.42, 27.23, 25.18, 21.20; MS (FAB) (M + Na)$^+$ 758.69.

(1*R*)-3-(3,4-Dimethoxyphenyl)-1-[3-(*t*-butoxycarbonylmethoxy)phenyl]-1-propyl (2*S*)-2-Piperidinecarboxylate (B). A solution of the above Fmoc-protected pipecolyl ester (833 mg, 1.13 mmol) in CH_2Cl_2 (30 mL) was treated with piperidine (1.12 mL, 11.3 mmol), and the mixture was stirred overnight at ambient temperature. The reaction mixture was concentrated and flash chromatographed (silica gel, 50 to 100% EtOAc/hexanes) to afford the free amine (569 mg, 98%) as a white sticky foam: IR (neat) 2935, 1748, 1590, 1516, 1453, 1153, 1030, 733 cm^{-1}; ^{1}H NMR ($CDCl_3$, 300 MHz) (mixture of rotamers, data for trans rotamer) 7.28 (t, J = 7.9 Hz, 1H), 6.98 (d, J = 7.7 Hz, 1H), 6.93 (s, 1H), 6.84 (m, 2H), 6.71 (d, J = 8.3 Hz, 1H), 6.69 (s, 1H), 5.77 (dd, J = 6.3, 6.8 Hz, 1H), 4.55 (s, 2H), 3.91 (s, 6H), 3.42 (m, 1H), 3.33 (s, 1H), 3.01 (m, 1H), 2.39−2.63 (m, 3H), 2.11−2.27 (m, 1H), 2.05−2.09 (m, 1H), 1.92 (m, 1H), 1.54 (s, 9H), 1.54−1.74 (m, 4H); ^{13}C NMR ($CDCl_3$, 75 MHz) 173.42, 168.29, 158.34, 149.20, 147.64, 142.54, 134.06, 129.92, 120.49, 120.19, 114.11, 113.54, 111.99, 111.60, 82.74, 75.21, 66.05, 61.45, 56.30, 56.21, 48.57, 38.55, 31.63, 29.41, 28.44, 25.70, 22.56; MS (FAB) (M + H)$^+$ 514.30.

General Procedure for 2-Alkyl Trimethoxyphenylacetic Acid Synthesis (C). Sodium bis(trimethylsilyl)amide (40 mL, 1.0 M solution in THF) was added slowly to a stirring solution of 3,4,5-trimethoxyphenylacetic acid (4.0 g, 17.7 mmol) in 20 mL of dry THF at 0 °C under nitrogen. After 15 min, alkyl bromide or iodide (21.3 mmol) was added. The solution was allowed to warm to room temperature. After 12 h, the mixture was diluted with 100 mL of ethyl acetate and acidified by careful addition of 60 mL of 1.0 N HCl. The layers were separated, and the aqueous phase was extracted with an

additional 50 mL of ethyl acetate. The organic portions were combined and washed with water (2 × 10 mL) and brine (10 mL), dried over anhydrous $MgSO_4$, concentrated, and subjected to flash chromatography (2.5% AcOH in 1:1 EtOAc/hexane) to yield the desired acid as a white solid.

2-Ethyl-(3,4,5-trimethoxyphenyl)acetic Acid. ^{1}H NMR ($CDCl_3$, 300 MHz) 6.53 (s, 2H), 3.85 (s, 6H), 3.83 (s, 3H), 3.39 (t, J = 7.6 Hz, 1H), 2.14−2.04 (m, 1H), 1.85−1.75 (m, 1H), 0.93 (t, J = 7.2 Hz, 3H); MS (ES)$^-$ 254.

2-Allyl-(3,4,5-trimethoxyphenyl)acetic Acid. ^{1}H NMR ($CDCl_3$, 300 MHz) 6.54 (s, 2H), 5.81−5.67 (m, 1H), 5.11 (d, J = 15.6 Hz, 1H), 5.07 (d, J = 6.9 Hz, 1H), 3.85 (s, 6H), 3.83 (s, 3H), 3.57 (dd, J = 7.0, 8.5 Hz, 1H), 2.85−2.75 (m, 1H), 2.56−2.47 (m, 1H); MS (FAB) (M − H)$^-$ 265.14.

2-Propyl-(3,4,5-trimethoxyphenyl)acetic Acid. ^{1}H NMR ($CDCl_3$, 300 MHz) 6.54 (s, 2H), 3.85 (s, 6H), 3.83 (s, 3H), 3.48 (t, J = 7.6 Hz, 1H), 2.07−2.01 (m, 1H), 1.78−1.71 (m, 1H), 1.37−1.26 (m, 2H), 0.98−0.86 (m, 3H); MS (FAB) (M − H)$^-$ 267.09.

2-Isopropyl-(3,4,5-trimethoxyphenyl)acetic Acid. ^{1}H NMR ($CDCl_3$, 300 MHz) 6.56 (s, 2H), 3.85 (s, 6H), 3.83 (s, 3H), 3.06 (d, J = 10.7 Hz, 1H), 2.33−2.23 (m, 1H), 1.08 (d, J = 6.5 Hz, 3H), 0.75 (d, J = 6.7 Hz, 3H); MS (FAB) (M − H)$^-$ 267.09.

2-Cyclopropylmethyl-(3,4,5-trimethoxyphenyl)acetic Acid. ^{1}H NMR ($CDCl_3$, 300 MHz) 11.32 (brs, 1H), 6.56 (s, 2H), 3.85 (s, 6H), 3.83 (s, 3H), 3.60 (t, J = 7.5 Hz, 1H), 1.95−1.68 (m, 2H), 0.43 (m, 2H), 0.13−0.02 (m, 2H).

General Procedure for Ligand Synthesis. A solution of the above amine (484 mg, 0.94 mmol) in CH_2Cl_2 (10 mL) was treated with the appropriate phenylacetic acid analogue (1.9 mmol) followed by PyBroP (878 mg, 1.9 mmol) and diisopropylethylamine (819 mL, 4.7 mmol) under a nitrogen atmosphere at ambient temperature. The resulting solution was allowed to stir overnight. The reaction mixture was then concentrated and flash chromatographed (silica gel, EtOAc/hexanes/CH_2Cl_2) to afford the penultimate *tert*-butyl ester-protected pipecolyl phenylacetamide as a white foam. A solution of the *tert*-butyl ester (0.48 mmol) in CH_2Cl_2 (4 mL) was treated with trifluoroacetic acid (0.74 mL, 9.6 mmol), and the mixture was stirred at ambient temperature for 2 h. The reaction mixture was then diluted with toluene (50 mL), concentrated, and flash chromatographed (silica gel, EtOAc with 1% acetic acid) to afford the acid as a white solid.

The diastereomeric *tert*-butyl ester precursors of compounds **8R** and **8S** and of **9R** and **9S** were prepared independently from enantiomerically pure α-methylphenylacetic acids or α-ethylphenylacetic acids, respectively. The diastereomeric pairs of all other *tert*-butyl ester precursors were prepared as mixtures from the corresponding racemic trimethoxyphenylactic acids or phenylacetic acids and separated by flash chromatography (as specified above) or by normal phase HPLC prior to TFA deprotection. The stereochemistries of each pair of diastereomers were assigned by comparison of their NMR spectra with those of **8** and **9**.

Compound homegeneity was assessed utilizing both normal and reverse phase HPLC analysis: normal phase HPLC (250 mm × 4.6 mm Chiralcel OD column, 35% 2-propanol:65% hexanes with 0.2% formic acid, 1.5 mL/min, ambient temperature, detection at 254 nm); reverse phase HPLC (250 mm × 4.6 mm Vydac 218TP54 column, gradient elution at 1 mL/min: 1 min- 55% A (90% CH_3CN/H_2O with 0.1% TFA), 45% B (H_2O with 0.1% TFA); 31 min- 80% A; 32 min- 100% A, column temperature of 60 °C, detection at 254 nm).

Compound 2S. IR (neat) 2939, 1741, 1591, 1515, 1454, 1241, 1128, 1027, 731 cm^{-1}; ^{1}H NMR ($CDCl_3$, 300 MHz) (mixture of rotamers) 7.19 (t, J = 7.9 Hz, 1H), 6.67−6.96 (m, 6H) 6.24 (s, 2H), 5.48−5.50 (m, 2H), 4.60−4.74 (m, 2H), 3.86 (s, 3H), 3.85 (s, 3H), 3.78 (s, 3H), 3.61−3.93 (m, 2H), 3.55 (s, 6H), 2.85−2.93 (m, 1H), 2.56−2.68 (m, 2H), 1.98−2.36 (m, 4H), 1.63−1.77 (m, 4H), 1.26−1.46 (m, 2H), 0.90 (t, J = 7.3 Hz, 3H); ^{13}C NMR ($CDCl_3$, 75 MHz) 174.2, 171.4, 170.6, 158.7, 153.7, 143.2, 135.1, 133.9, 130.0, 120.8, 120.0, 116.4, 112.3, 112.0, 105.4, 77.8, 66.2, 61.3, 56.5, 52.9, 51.7, 39.0, 32.1, 28.7, 27.8, 25.7, 21.4, 12.0; HRMS (FAB) (M + H)$^+$ calc. 694.3227, meas. 694.3197; HPLC retention time = 10.89 min (normal phase), 7.24 min (reverse phase).

Compound 2R. IR (neat) 2939, 1738, 1590, 1514, 1454, 1240, 1129, 1017, 913, 731 cm^{-1}; ^{1}H NMR ($CDCl_3$, 300 MHz) (mixture of rotamers) 7.25 (t, J = 7.8 Hz, 1H), 6.70−6.90 (m, 6H), 6.45 (s, 2H), 5.66−5.70 (m, 1H), 5.53 (d, J = 4.5 Hz, 1H), 4.59−4.72 (m, 2H), 3.86 (s, 3H), 3.85 (s, 3H), 3.84 (s, 3H), 3.83 (s, 6H), 3.47−3.79 (m, 2H), 3.23−3.32 (m, 1H), 2.52−2.71 (m, 2H), 2.00−2.31 (m, 4H), 1.52−1.75 (m, 4H), 1.28−1.46 (m, 2H), 0.83 (t, J = 7.3 Hz, 3H); ^{13}C NMR ($CDCl_3$, 75 MHz) 174.3, 172.0, 171.0, 158.6, 154.0, 149.6, 148.1, 142.7, 137.6, 136.3, 134.0, 130.3, 120.8, 120.2, 116.2, 112.3, 112.0, 110.9, 105.5, 77.8, 77.1, 66.0, 61.5, 56.9, 56.6, 56.5, 53.2, 51.6, 44.0, 38.7, 32.0, 28.4, 27.5, 25.4, 21.5, 12.9; HRMS (FAB) (M + H)$^+$ calc. 694.3227, meas. 694.3245; HPLC retention time = 13.64 min (normal phase), 7.09 min (reverse phase).

Compound 3S. IR (neat) 2939, 1739, 1590, 1514, 1453, 1240, 1127 cm^{-1}; ^{1}H NMR ($CDCl_3$, 300 MHz) (mixture of rotamers) 7.19 (t, J = 7.8 Hz, 1H), 6.84−6.66 (m, 6H), 6.44 (brs, 1H), 6.33 (s, 2H), 5.84−5.71 (m, 1H), 5.56 (dd, J = 5.1, 8.5 Hz, 1H), 5.47 (d, J = 5.6 Hz, 1H), 5.04 (d, J = 18.3 Hz, 1H), 4.99 (d, J = 10.1 Hz, 1H), 4.65 (AB, J = 16.4 Hz, 2H), 3.85 (s, 3H), 3.84 (s, 3H), 3.92−3.67 (m, 2H), 3.78 (s, 3H), 3.61 (s, 6H), 2.92−2.76 (m, 2H), 2.65−2.30 (m, 4H), 2.21−1.95 (m, 2H), 1.76−1.42 (m, 5H); ^{13}C NMR ($CDCl_3$, 75 MHz) 173.2, 171.8, 170.6, 158.4, 153.6, 149.4, 147.8, 142.8, 137.1, 136.8, 134.5, 133.8, 129.9, 120.6, 119.8, 116.8, 115.4, 112.2, 111.8, 110.8, 105.4, 76.8, 65.7, 61.1, 56.5, 56.3, 52.7, 49.8, 43.9, 39.7, 38.7, 32.0, 27.4, 25.6, 21.2; HRMS (FAB) (M + H)$^+$ calc. 706.3227, meas. 706.3249; HPLC retention time = 10.91 min (normal phase), 10.24 min (reverse phase).

Compound 3R. IR (neat) 2937, 1737, 1590, 1512, 1453, 1239, 1128 cm^{-1}; ^{1}H NMR ($CDCl_3$, 300 MHz) (mixture of rotamers) 7.26 (t, J = 8.9 Hz, 1H), 6.94−6.68 (m, 7H), 6.47 (s, 2H), 5.79−5.67 (m, 2H), 5.54 (d, J = 4.4 Hz, 1H), 5.00 (dd, J = 1.4, 17.1 Hz, 1H), 4.93 (d, J = 10.2 Hz, 1H), 4.65 (s, 2H), 3.86−3.61 (m, 17H), 3.22 (dt, J = 2.3, 12.0 Hz, 1H), 2.86−2.81 (m, 1H), 2.79−2.33 (m, 3H), 2.31−2.04 (m, 3H), 1.63−1.30 (m, 5H); ^{13}C NMR ($CDCl_3$, 75 MHz) 173.2, 172.1, 170.9, 158.4, 153.8, 149.4, 147.8, 142.4, 137.5, 136.5, 135.6, 133.8, 130.1, 120.6, 120.1, 116.9, 115.3, 112.2, 112.0, 111.9, 105.3, 76.7, 65.6, 61.3, 56.7, 56.3, 53.0, 49.7, 43.8, 39.3, 38.5, 32.0, 27.1, 25.1, 23.0, 21.2; HRMS (FAB) (M + H)$^+$ calc. 706.3227, meas. 706.3210; HPLC retention time = 13.59 min (normal phase), 10.11 min (reverse phase).

Compound 4S. IR (neat) 2938, 1739, 1590, 1514, 1454, 1240, 1128, 1027 cm^{-1}; ^{1}H NMR ($CDCl_3$, 300 MHz) (mixture of rotamers) 9.53 (brs, 1H), 7.16 (t, J = 7.9 Hz, 1H), 6.86−6.64 (m, 6H), 6.30 (s, 2H), 5.53 (dd, J = 5.0, 8.4 Hz, 1H), 5.46 (d, J = 4.8 Hz, 1H), 4.63 (AB, J = 16.4 Hz, 2H), 3.83 (s, 3H), 3.82 (s, 3H), 3.79−3.64 (m, 2H), 3.76 (s, 3H), 3.59 (s, 6H), 2.85 (t, J = 13.1 Hz, 1H), 2.65−2.45 (m, 2H), 2.31 (d, J = 13.1 Hz, 1H), 2.17−1.95 (m, 3H), 1.72−1.51 (m, 4H), 1.44−1.24 (m, 4H), 0.88 (t, J = 7.3 Hz, 3H); ^{13}C NMR ($CDCl_3$, 75 MHz) 173.9, 171.9, 170.6, 158.4, 153.6, 149.4, 147.8, 142.8, 136.4, 135.4, 133.8, 129.9, 120.6, 119.9, 115.4, 112.2, 111.8, 110.8, 105.3, 76.7, 65.8, 61.1, 56.3, 52.7, 49.4, 43.9, 38.6, 37.7, 31.8, 27.4, 25.6, 21.4, 14.4; HRMS (FAB) (M + H)$^+$ calc. 708.3384, meas. 708.3365; HPLC retention time = 9.55 min (normal phase), 10.75 min (reverse phase).

Compound 4R. IR (neat) 2936, 1738, 1590, 1514, 1455, 1330, 1240, 1128, 1012 cm^{-1}; ^{1}H NMR ($CDCl_3$, 300 MHz) (mixture of rotamers) 9.98 (brs, 1H), 7.23 (t, J = 7.7 Hz, 1H), 6.91−6.65 (m, 6H), 6.45 (s, 2H), 5.71 (dd, J = 5.4, 7.9 Hz, 1H), 5.53 (d, J = 4.4 Hz, 1H), 4.62 (s, 2H), 3.83 (s, 6H), 3.80 (s, 9H), 3.75−3.59 (m, 2H), 3.19 (dt, J = 13.0, 2.1 Hz, 1H), 2.61−2.50 (m, 2H), 2.28−2.17 (m, 2H), 2.10−1.97 (m, 2H), 1.70−1.17 (m, 8H), 0.84 (t, J = 7.3 Hz, 3H); ^{13}C NMR ($CDCl_3$, 75 MHz) 173.9, 172.0, 170.9, 158.4, 153.8, 149.3, 147.8, 142.4, 137.3, 136.4, 133.9, 130.1, 120.6, 120.0, 115.2, 112.2, 112.1, 111.9, 105.3, 76.9, 65.6, 61.2, 56.7, 56.3, 52.9, 49.2, 43.9, 39.3, 38.4, 37.3, 31.7, 27.1, 25.2, 21.3, 14.4; HRMS (FAB) (M + H)$^+$ calc. 708.3384, meas. 708.3382; HPLC retention time = 12.70 min (normal phase), 11.27 min (reverse phase).

Compound 5S. IR (neat) 2938, 1737, 1590, 1513, 1455, 1240, 1128, 1025 cm^{-1}; ^1H NMR ($CDCl_3$, 300 MHz) (mixture of rotamers) 7.16 (t, J = 8.0 Hz, 1H), 6.94−6.45 (m, 6H), 6.33 (s, 2H), 5.51 (dd, J = 5.0, 8.5 Hz, 1H), 5.46 (d, J = 4.1 Hz, 1H), 4.63 (AB, J = 16.3 Hz, 2H), 3.85−3.73 (m, 13H), 3.60 (s, 3H), 3.27 (d, J = 9.2 Hz, 1H), 2.86 (t, J = 13.0 Hz, 1H), 2.61−2.26 (m, 4H), 2.16−1.92 (m, 2H), 1.74−1.26 (m, 5H), 1.00 (d, J = 6.2 Hz, 3H), 0.70 (d, J = 6.7 Hz, 3H); ^{13}C NMR ($CDCl_3$, 75 MHz) 173.4, 171.0, 170.0, 158.1, 153.0, 149.0, 147.5, 142.6, 136.9, 133.4, 133.2, 129.6, 120.3, 119.6, 115.5, 111.8, 111.5, 109.5, 105.9, 76.4, 65.7, 60.9, 56.6, 56.1, 52.4, 43.6, 38.3, 31.9, 31.5, 27.3, 25.4, 22.3, 20.9, 20.4; HRMS (FAB) $(M + H)^+$ calc. 708.3384, meas. 708.3361; HPLC retention time = 7.69 min (normal phase), 8.27 min (reverse phase).

Compound 5R. IR (neat) 2939, 1736, 1590, 1514, 1458, 1239, 1129, 1021 cm^{-1}; ^1H NMR ($CDCl_3$, 300 MHz) (single enantiomer, mixture of rotamers) 7.24 (t, J = 7.9 Hz, 1H), 6.91−6.67 (m, 6H), 6.50 (s, 2H), 5.71 (dd, J = 5.0, 8.0 Hz, 1H), 5.52 (d, J = 4.3 Hz, 1H), 4.64 (s, 2H), 4.69−4.57 (br, 1H), 4.00 (d, J = 12.0 Hz, 1H), 3.85−3.60 (m, 6H), 3.32−3.28 (m, 2H), 2.65−2.56 (m, 2H), 2.38−2.05 (m, 4H), 1.65−1.27 (m, 4H), 0.99 (m, 1H), 0.94 (d, J = 6.3 Hz, 3H), 0.68 (d, J = 6.6 Hz, 3H); ^{13}C NMR ($CDCl_3$, 75 MHz) 173.7, 171.8, 170.5, 158.1, 153.3, 149.0, 147.5, 142.1, 137.1, 134.7, 133.5, 129.7, 120.2, 119.6, 115.4, 111.8, 111.5, 110.7, 105.3, 76.3, 65.7, 60.9, 56.0, 55.9, 52.6, 43.7, 38.1, 32.2, 31.5, 26.7, 24.9, 22.1, 20.9, 20.4; HRMS (FAB) $(M + H)^+$ calc. 708.3384, meas. 708.3402; HPLC retention time = 11.21 min (normal phase), 8.32 min (reverse phase).

Compound 6S. IR (neat) 2938, 1740, 1590, 1514, 1453, 1239, 1126, 1026 cm^{-1}; ^1H NMR ($CDCl_3$, 300 MHz) (mixture of rotamers) 10.48 (brs, 1H), 7.18 (t, J = 7.9 Hz, 1H), 6.84−6.65 (m, 6H), 6.35 (s, 2H), 5.56 (dd, J = 5.0, 8.4 Hz, 1H), 5.49 (d, J = 4.5 Hz, 1H), 4.66 (AB, J = 18.7 Hz, 2H), 3.85 (s, 3H), 3.84 (s, 3H), 3.83−3.80 (m, 2H), 3.78 (s, 3H), 3.61 (s, 6H), 2.88 (dt, J = 2.5, 13.4 Hz, 1H), 2.64−2.49 (m, 2H), 2.33 (d, J = 13.4 Hz, 1H), 2.18−1.93 (m, 3H), 1.76−1.42 (m, 6H), 0.70−0.66 (m, 1H), 0.42−0.39 (m, 2H), 0.07−0.02 (m, 2H); ^{13}C NMR ($CDCl_3$, 75 MHz) 173.9, 172.4, 170.6, 158.4, 153.5, 149.4, 147.8, 142.8, 137.1, 135.2, 133.8, 129.9, 120.6, 119.9, 115.4, 112.2, 111.8, 110.9, 105.4, 76.7, 65.7, 61.1, 56.3, 52.7, 49.9, 43.9, 40.5, 38.6, 31.8, 27.4, 25.6, 21.2, 9.7, 5.2, 4.9; HRMS (FAB) $(M + H)^+$ calc. 720.3384, meas. 720.3417; HPLC retention time = 10.66 min (normal phase), 9.02 min (reverse phase).

Compound 6R. IR (neat) 2937, 1738, 1590, 1514, 1453, 1239, 1127, 1015 cm^{-1}; ^1H NMR ($CDCl_3$, 300 MHz) (mixture of rotamers) 9.58 (brs, 1H), 7.24 (t, J = 7.8 Hz, 1H), 6.92−6.67 (m, 6H), 6.49 (s, 2H), 5.71 (dd, J = 5.3, 8.0 Hz, 1H), 5.55 (d, J = 3.8 Hz, 1H), 4.62 (s, 2H), 3.94−3.60 (m, 17H), 3.26 (t, J = 11.0 Hz, 1H), 2.67−2.55 (m, 2H), 2.31−2.16 (m, 2H), 2.10−1.86 (m, 2H), 1.63−1.25 (m, 5H), 0.91−0.82 (m, 1H), 0.59 (m, 1H), 0.35−0.32 (m, 2H), 0.01−0.00 (m, 2H); ^{13}C NMR ($CDCl_3$, 75 MHz) 173.7, 172.3, 170.5, 158.0, 153.6, 148.9, 147.4, 142.1, 137.0, 135.9, 133.4, 129.7, 120.2, 119.7, 115.0, 111.8, 111.5, 105.0, 76.4, 65.5, 60.9, 56.3, 55.9, 52.7, 49.6, 43.6, 39.7, 38.1, 31.4, 29.7, 26.8, 24.7, 9.2, 4.8, 4.4; HRMS (FAB) $(M + H)^+$ calc. 720.3384, meas. 720.3401; HPLC retention time = 13.25 min (normal phase), 8.75 min (reverse phase).

Compound 7. IR (neat) 2938, 1736, 1593, 1516, 1452, 1237, 1156, 1027, 732, 698 cm^{-1}; ^1H NMR ($CDCl_3$, 300 MHz) (mixture of rotamers) 7.26−7.20 (m, 6H), 6.91−6.77 (m, 4H), 6.70−6.64 (m, 3H), 5.68 (dd, J = 5.1, 6.0 Hz, 1H), 5.48 (s, 1H), 4.59 (AB, J = 16.4 Hz, 2H), 3.85 (s, 6H), 3.77−3.73 (m, 3H), 3.24 (t, J = 11.7 Hz, 1H), 2.65−2.50 (m, 2H), 2.32 (d, J = 12.4 Hz, 1H), 2.24−2.03 (m, 3H), 1.69−1.56 (m, 3H), 1.33−1.25 (m, 2H); ^{13}C NMR ($CDCl_3$, 75 MHz) 172.1, 171.9, 170.7, 158.5, 149.4, 147.9, 142.4, 134.9, 133.9, 130.1, 129.1, 129.0, 127.2, 120.6, 120.0, 115.7, 112.3, 111.9, 111.4, 76.8, 65.8, 56.4, 56.3, 52.8, 44.5, 41.4, 38.4, 31.8, 27.2, 25.4, 21.1; HRMS (FAB) $(M + H)^+$ calc. 576.2597, meas. 576.2623; HPLC retention time = 18.67 min (normal phase), 7.80 min (reverse phase).

Compound 8S. IR (neat) 2936, 1736, 1598, 1516, 1450, 1238, 1158, 1027 cm^{-1}; ^1H NMR ($CDCl_3$, 300 MHz) (mixture of rotamers) 10.17 (brs, 1H), 7.32−7.14 (m, 6H), 6.96−6.67 (m, 6H), 5.69 (dd, J = 5.2, 7.6 Hz, 1H), 5.52 (s, 1H), 4.58 (s, 2H), 3.94 (q, J = 6.7 Hz, 1H), 3.84 (s, 6H), 3.76 (d, J = 12.6 Hz, 1H), 2.75 (t, J = 11.5 Hz, 1H), 2.62−2.46 (m, 2H), 2.34−2.02 (m, 3H), 1.99−1.27 (m, 5H), 0.88 (m, 3H); ^{13}C NMR ($CDCl_3$, 75 MHz) 174.1, 172.2, 170.7, 158.2, 149.4, 147.8, 142.4, 141.5, 134.0, 130.0, 129.3, 127.8, 127.4, 127.2, 120.6, 120.2, 115.4, 112.3, 111.9, 76.4, 65.7, 56.4, 56.3, 52.8, 44.1, 43.8, 38.4, 32.0, 27.2, 25.6, 21.3, 21.2; HRMS (FAB) $(M + H)^+$ calc. 590.2754, meas. 590.2745; HPLC retention time = 11.03 min (normal phase), 7.38 min (reverse phase).

Compound 8R. IR (neat) 2937, 1737, 1604, 1516, 1452, 1238, 1158, 10278, 701 cm^{-1}; ^1H NMR ($CDCl_3$, 300 MHz) (mixture of rotamers) 9.73 (brs, 1H), 7.33−7.08 (m, 6H), 6.91−6.68 (m, 6H), 5.69 (dd, J = 5.1, 8.3 Hz, 1H), 5.54 (d, J = 4.1 Hz, 1H), 4.64 (d, J = 4.4 Hz, 2H), 3.89 (q, J = 6.6 Hz, 1H), 3.85 (s, 3H), 3.83 (s, 3H), 3.75 (d, J = 12.3 Hz, 1H), 3.23 (dt, J = 2.3, 12.9 Hz, 1H), 2.71−2.51 (m, 2H), 2.30−2.17 (m, 2H), 2.12−2.03 (m, 1H), 1.71−1.27 (m, 8H); ^{13}C NMR ($CDCl_3$, 75 MHz) 174.6, 172.1, 170.9, 158.5, 149.4, 147.9, 142.5, 142.3, 133.9, 130.1, 129.4, 127.6, 127.2, 120.6, 120.0, 115.8, 112.3, 111.9, 111.1, 76.8, 65.8, 56.4, 56.3, 53.0, 44.0, 43.7, 38.5, 31.8, 27.2, 24.9, 21.3, 20.9; HRMS (FAB) $(M + H)^+$ calc. 590.2754, meas. 590.2776; HPLC retention time = 21.02 min (normal phase), 13.58 min (reverse phase).

Compound 9S. IR (neat) 2938, 1735, 1596, 1516, 1452, 1237, 1158, 1026, 701 cm^{-1}; ^1H NMR ($CDCl_3$, 300 MHz) (mixture of rotamers) 9.66 (brs, 1H), 7.28−7.13 (m, 7H), 7.00−6.62 (m, 5H), 5.69 (t, J = 6.6 Hz, 1H), 5.54 (brs, 1H), 4.59 (s, 2H), 3.87 (s, 6H), 3.70 (t, J = 7.0 Hz, 1H), 2.80−2.09 (m, 7H), 1.98−1.17 (m, 7H), 0.90 (m, 3H); ^{13}C NMR ($CDCl_3$, 75 MHz) 173.4, 172.3, 170.7, 158.1, 149.4, 147.8, 142.4, 139.7, 134.0, 130.0, 129.4, 129.1, 128.5, 127.3, 120.7, 120.3, 115.1, 112.4, 111.9, 76.4, 65.6, 56.4, 56.3, 52.7, 51.1, 44.1, 38.4, 31.7, 28.5, 27.2, 25.7, 21.3, 12.7; HRMS (FAB) (M + Na) calc. 626.2730, meas. 626.2733; HPLC retention time = 9.12 min (normal phase), 9.64 min (reverse phase).

Compound 9R. IR (neat) 2937, 1737, 1596, 1516, 1451, 1237, 1158, 1026, 701 cm^{-1}; ^1H NMR ($CDCl_3$, 300 MHz) (mixture of rotamers) 10.15 (s, 1H), 7.32−7.21 (m, 6H), 7.09−6.57 (m, 6H), 5.73 (dd, J = 5.4, 7.9 Hz, 1H), 5.56 (s, 1H), 4.65 (s, 2H), 3.85 (s, 3H), 3.83 (s, 3H), 3.64 (t, J = 7.1 Hz, 1H), 3.20 (t, J = 12.7 Hz, 1H), 2.69−2.51 (m, 2H), 2.27−2.03 (m, 4H), 1.86−1.27 (m, 7H), 0.95−0.81 (m, 3H); ^{13}C NMR ($CDCl_3$, 75 MHz) 176.9, 174.0, 172.3, 158.4, 149.4, 147.8, 142.4, 140.5, 133.9, 130.1, 129.1, 128.2, 127.3, 120.6, 120.1, 115.3, 112.0, 111.9, 76.7, 65.7, 56.3, 56.2, 52.9, 51.2, 43.8, 38.5, 31.9, 28.2, 27.0, 25.6, 21.3, 12.6; HRMS (FAB) (M + Na) calc. 626.2730, meas. 626.2700; HPLC retention time = 15.67 min (normal phase), 10.78 min (reverse phase).

Compound 10S. IR (neat) 2956, 1733, 1594, 1516, 1453, 1236, 1158, 1026 cm^{-1}; ^1H NMR ($CDCl_3$, 300 MHz) (mixture of rotamers) 7.29−6.55 (m, 12H), 5.60 (dd, J = 5.3, 8.2 Hz, 1H), 5.47 (d, J = 4.6 Hz, 1H), 4.60 (d, J = 2.9 Hz, 2H), 3.95 (d, J = 13.8 Hz, 1H), 3.84 (s, 6H), 3.37 (d, J = 9.6 Hz, 1H), 2.80 (t, J = 12.0 Hz, 1H), 2.58−2.24 (m, 4H), 2.09−1.85 (m, 2H), 1.69−1.37 (m, 4H), 1.02 (d, J = 6.4 Hz, 3H), 0.67 (d, J = 6.7 Hz, 3H); ^{13}C NMR ($CDCl_3$, 75 MHz) 173.0, 171.5, 170.2, 157.7, 148.9, 147.4, 142.2, 138.1, 133.6, 129.6, 128.7, 128.5, 128.1, 127.0, 120.3, 119.8, 115.0, 111.9, 111.4, 75.9, 65.3, 56.4, 56.0, 55.9, 52.3, 43.7, 37.9, 32.1, 31.3, 27.0, 25.4, 22.2, 21.0, 20.3; HRMS (FAB) $(M + H)^+$ calc. 618.3067, meas. 618.3088; HPLC retention time = 8.22 min (normal phase), 12.59 min (reverse phase).

Compound 10R. IR (neat) 2937, 1737, 1594, 1515, 1452, 1236, 1158, 1026 cm^{-1}; ^1H NMR ($CDCl_3$, 300 MHz) (mixture of rotamers) 8.13 (brs, 1H), 7.27−7.22 (m, 6H), 6.92−6.67 (m, 6H), 5.72 (dd, J = 5.2, 8.0 Hz, 1H), 5.52 (d, J = 4.3 Hz, 1H), 4.59 (d, J = 10.9 Hz, 2H), 3.97 (d, J = 10.9 Hz, 1H), 3.86 (s, 3H), 3.84 (s, 3H), 3.39 (d, J = 9.7 Hz, 1H), 3.26 (t, J = 11.8 Hz, 1H), 2.70−2.52 (m, 2H), 2.48−2.35 (m, 1H), 2.26−2.16 (m, 2H), 2.13−2.03 (m, 1H), 1.59−1.42 (m, 4H), 0.96 (d, J = 6.4 Hz, 3H), 0.65 (d, J = 6.7 Hz, 3H); ^{13}C NMR ($CDCl_3$, 75 MHz) 173.8, 171.6, 170.4, 158.0, 149.0, 147.4, 142.1, 139.0, 133.5, 129.7, 128.6, 128.5, 127.0, 120.2, 119.7, 115.4, 111.8, 111.4, 110.6, 76.3, 65.4, 56.3, 55.9, 55.8, 52.5, 43.6, 38.1, 32.0, 31.4,

26.7, 24.8, 22.2, 20.9, 20.4; HRMS (FAB) $(M + H)^+$ calc. 618.3067, meas. 618.3045; HPLC retention time = 12.00 min (normal phase), 12.44 min (reverse phase).

Compound 11S. IR (neat) 2999, 1734, 1594, 1516, 1450, 1158, 1028, 700 cm^{-1}; ^1H NMR ($CDCl_3$, 300 MHz) (mixture of rotamers) 7.26−7.12 (m, 6H), 6.98−6.56 (m, 6H), 5.58 (dd, J = 4.8, 8.0 Hz, 1H), 5.47 (s, 1H), 4.61 (AB, J = 15.4 Hz, 2H), 3.96 (d, J = 13.6 Hz, 1H), 3.85 (s, 6H), 3.46 (d, J = 9.7 Hz, 1H), 2.82 (t, J = 12.2 Hz, 1H), 2.59−2.41 (m, 2H), 2.32−1.92 (m, 5H), 1.89−1.42 (m, 6H), 1.26−0.67 (m, 8H); ^{13}C NMR ($CDCl_3$, 75 MHz) 173.0, 170.2, 157.7, 148.9, 147.4, 142.2, 137.6, 133.6, 129.6, 128.8, 128.5, 126.9, 120.3, 119.8, 115.2, 111.9, 111.4, 111.1, 75.9, 56.0, 55.1, 52.4, 43.7, 41.2, 37.9, 32.8, 31.6, 30.7, 27.0, 26.5, 26.2, 25.5, 21.0; HRMS (FAB) $(M + H)^+$ calc. 658.3380, meas. 658.3398; HPLC retention time = 8.19 min (normal phase), 17.24 min (reverse phase).

Compound 11R. IR (neat) 2931, 1737, 1595, 1516, 1449, 1236, 1158, 1028, 701 cm^{-1}; ^1H NMR ($CDCl_3$, 300 MHz) (mixture of rotamers) 7.27−7.16 (m, 6H), 6.90−6.48 (m, 6H), 5.68 (dd, J = 4.6, 7.9 Hz, 1H), 5.51 (s, 1H), 4.69 (AB, J = 16.8 Hz, 2H), 3.96 (d, J = 12.8 Hz, 1H), 3.87 (s, 3H), 3.86 (s, 3H), 3.46 (d, J = 9.7 Hz, 1H), 3.30 (t, J = 12.3 Hz, 1H), 2.68−2.53 (m, 2H), 2.27−2.08 (m, 4H), 1.82−1.44 (m, 7H), 1.26−1.06 (m, 4H), 0.98−0.68 (m, 4H); ^{13}C NMR ($CDCl_3$, 75 MHz) 173.9, 170.4, 158.1, 149.0, 147.5, 142.2, 138.4, 133.5, 129.7, 128.6, 128.5, 126.9, 120.2, 119.6, 115.9, 111.8, 111.4, 109.7, 76.4, 55.9, 55.1, 52.6, 43.6, 41.1, 38.1, 32.7, 31.5, 30.7, 26.8, 26.5, 26.1, 24.9, 20.9; HRMS (FAB) $(M + H)^+$ calc. 658.3380, meas. 658.3349; HPLC retention time = 10.47 min (normal phase), 18.25 min (reverse phase).

Compound 12. IR (neat) 2937, 1735, 1599, 1515, 1453, 1236, 1157, 1025, 700 cm^{-1}; ^1H NMR ($CDCl_3$, 300 MHz) (mixture of rotamers) 7.33−7.07 (m, 11H), 6.95−6.67 (m, 6H), 6.17 (brs, 1H), 5.71 (dd, J = 5.1, 8.0 Hz, 1H), 5.53 (d, J = 3.4 Hz, 1H), 5.24 (s, 1H), 4.55 (AB, J = 16.6 Hz, 2H), 3.85 (s, 7H), 3.18 (t, J = 12.0 Hz, 1H), 2.66−2.56 (m, 2H), 2.35−2.08 (m, 3H), 1.70−1.53 (m, 3H), 1.49−1.26 (m, 2H); ^{13}C NMR ($CDCl_3$, 75 MHz) 172.4, 171.3, 170.4, 158.0, 149.0, 147.5, 142.1, 139.1, 138.8, 133.5, 129.1, 128.6, 128.5, 127.0, 120.2, 119.6, 115.5, 111.8, 111.4, 76.3, 65.2, 56.0, 55.9, 52.7, 44.0, 38.2, 31.5, 27.0, 25.0, 20.8; HRMS (FAB) $(M + H)^+$ calc. 652.2910, meas. 652.2934; HPLC retention time = 14.30 min (normal phase), 13.73 min (reverse phase).

FKBP Binding Assay. The affinities of synthetic ligands for FKBP12 were determined using a competitive assay based on fluorescence polarization (FP). Full details of the assay will be provided elsewhere (C. T. Rollins, E. Laborde, D. Holt, and T. Clackson, in preparation). Briefly, a fluorescent probe was prepared by coupling 4′-(aminomethyl)-fluorescein (Molecular Probes) to the modified allyl group of FK506 in a manner similar to the preparation of FK1012.[14] Recombinant human FKBP12 was expressed and purified by standard methods.[24] In the wells of a Dynatech microfluor plate, subsaturating concentrations of FKBP12 or F36V-FKBP were incubated with 2.5 nM probe and serial dilutions of competitive ligand in FP buffer (50 mM potassium phosphate pH 7.8/150 mM NaCl/100 μg/mL bovine gamma globulin/1% EtOH). After equilibration for 30 min in the dark, fluorescence polarization was read on a Jolley FPM-2 (Jolley Consulting and Research, Inc., Grayslake, IL). The increase in polarization of the probe upon binding protein was used as a direct readout of percent probe bound, compared to controls containing no competitor (100%) and no protein (0%), and the concentration of competitor resulting in 50% binding (IC_{50}) was determined by a nonlinear least-squares fit to a four-parameter equation.

Preparation of Uniformly [^{13}C]- and [^{15}N]-Labeled FKBP for NMR. Human F36V-FKBP with no hexahistidine-tag was produced in *Escherichia coli* BL21(DE3) from vector pET20b (Novagen Inc., Madison, WI).[9] Cells were grown at 37 °C in M9 medium containing 200 mg/L ampicillin, with U-[^{13}C]-D-glucose (2.9 g/L) and $^{15}NH_4Cl$ (1 g/L) (Cambridge Isotope Laboratories, Andover, MA), as the only carbon and nitrogen source, and they were induced at an A_{600} of approximately 0.8 with 1 mM isopropyl-β-D-thiogalactoside for 4−6 h at 25 °C. For purification, frozen cell paste was rapidly thawed into 5 volumes of chilled lysis buffer (20 mM Tris/Tris-HCl pH 7.4, containing 5 mM DTT, 5 mM EDTA, and 1 mM of the protease inhibitor AEBSF) (Calbiochem, San Diego, CA). The lysate was rapidly refrozen in an ethanol/dry ice bath and rapidly rethawed on a chilled water bath. The suspension was then centrifuged at 25000*g* for 15 min at 4 °C. After the solution was filtered through a 0.45 mm membrane, the clarified supernatant was loaded onto a polyethyleneimine column (3.3 mL of resin/g of cell paste) (Bakerbond PEI, VWR Scientific Products, Edison, NJ) and then a Macro-Prep High Q column (0.6 mL of resin/g of cell paste) (BioRad Laboratories, Hercules, CA), both columns having been equilibrated in lysis buffer. The flow-through was collected, concentrated on an Amicon YM3 membrane to 10−20 mg/mL, filtered through a 0.2 mm filter, and further purified by gel filtration on a 2.6 × 90 cm Sephacryl S100HR column (Pharmacia Biotech, Piscataway, NJ) equilibrated with 50 mM potassium phosphate buffer pH 6.5, containing 100 mM NaCl, 1 mM EDTA, 0.02% NaN_3, and 5 mM DTT, at a flow-rate of 1 mL/min. F36V-FKBP eluted at 345 mL, and the yield was approximately 8.5 mg/L culture.

NMR Methods and Structure Determination. The sequential NMR assignments of the protein were carried out using standard multidimensional heteronuclear NMR methods on a 1:1 double-labeled F36V-FKBP/ligand complex.[25] The two-dimensional ^1H-^{15}N HSQC[26] spectrum of uncomplexed double-labeled F36V-FKBP showed many broad peaks which sharpened upon adding ligand, suggesting that the uncomplexed protein may exist in some form of oligomerization equilibrium. However, F36V-FKBP migrated identically to WT FKBP in HPLC gel filtration on a TSK G2000SW column (7.5 × 300 mm, 5 mm particle size) (Tosohaas Inc., Montgomeryville, PA). By this criterion, F36V-FKBP was 97% monomeric following NMR analysis at 1−2 mM concentration at 30 °C, then dilution to 0.2 mM for injection on the TSK column. Therefore, any oligomerization phenomenon that might be responsible for line broadening of the uncomplexed protein in NMR appears to be of low affinity and rapidly reversible. Nevertheless, the effect was such that the sequential NMR assignment of the uncomplexed protein could not be completed for all of the residues.

Ligand−protein and ligand−ligand NOEs were obtained using isotope-filtered NMR methods.[27] The structures were calculated using a slow cooling simulated annealing docking procedure within X-PLOR in which protein−ligand and ligand−ligand NOEs (typically 60−70 and 20−25, respectively, for each complex) were used.[28] All the heavy atoms of the protein, with the exception of several side chains which showed NOEs to ligand, were held rigid. The starting coordinates were from the X-ray crystal structure of the F36V-FKBP/**2S** complex.[9] All the waters were removed, as the binding cavity does not contain any water molecules. A family of 15 structures, usually from a pool of 100−200 structures, which had minimum energy and showed no violations of the experimental NMR data and covalent geometries was selected. The rmsd was calculated for the heavy atoms of the ligand. The structure with a minimum violation energy among a family of structures was selected for comparison and overlay.

Acknowledgment. We thank Don Cullis and Bonnie Marmor for technical assistance in preparative chemistry and mass spectrometry.

Supporting Information Available: Tables of atomic coordinates for F36V-FKBP complexes with **2R**, **2S**, **9R**, **9S**, **10R**, and **10S** (PDB). This material is available free of charge via the Internet at http://pubs.acs.org.

References

(1) Babine, R. E.; Bender, S. L. Molecular Recognition of Protein−Ligand Complexes: Applications to Drug Design. *Chem. Rev.* **1997**, *97*, 1359−1472.

(2) Shah, K.; Liu, Y.; Deirmengian, C.; Shokat, K. M. Engineering Unnatural Nucleotide Specificity for Rous Sarcoma Virus Tyrosine Kinase to Uniquely Label Its Direct Substrates. *Proc. Natl. Acad. Sci. U.S.A.* **1997**, *94*, 3565−3570.

(3) Bishop, A. C.; Kung, C.-y.; Shah, K.; Witucki, L.; Shokat, K. M.; Liu, Y. Generation of Monospecific Nanomolar Tyrosine Kinase Inhibitors via a Chemical Genetic Approach. *J. Am. Chem. Soc.* **1999**, *121*, 627−631.
(4) Liu, Y.; Shah, K.; Yang, F.; Witucki, L.; Shokat, K. M. A Molecular Gate Which Controls Unnatural ATP Analogue Recognition by the Tyrosine Kinase v-Src. *Bioorg. Med. Chem.* **1998**, *6*, 1219−1226.
(5) Liu, Y.; Shah, K.; Yang, F.; Witucki, L.; Shokat, K. M. Engineering Src Family Protein Kinases with Unnatural Nucleotide Specificity. *Chem. Biol.* **1998**, *5*, 91−101.
(6) Bishop, A. C.; Shah, K.; Liu, Y.; Witucki, L.; Kung, C.-y.; Shokat, K. M. Design of Allele-Specific Inhibitors to Probe Protein Kinase Signaling. *Curr. Biol.* **1998**, *8*, 257−266.
(7) Belshaw, P. J.; Schoepfer, J. G.; Liu, K.-Q.; Morrison, K. L.; Schreiber, S. L. Rational Design of Orthogonal Receptor−Ligand Combinations. *Angew. Chem., Int. Ed. Engl.* **1995**, *34*, 2129−2132.
(8) Belshaw, P. J.; Schreiber, S. L. Cell-Specific Calcineurin Inhibition by a Modified Cyclosporin. *J. Am. Chem. Soc.* **1997**, *119*, 1805−1806.
(9) Clackson, T.; Yang, W.; Rozamus, L. W.; Hatada, M.; Amara, J. F.; Rollins, C. T.; Stevenson, L. F.; Magari, S. R.; Wood, S. A.; Courage, N. L.; Lu, X.; Cerasoli, F., Jr.; Gilman, M.; Holt, D. A. Redesigning an FKBP−Ligand Interface to Generate Chemical Dimerizers with Novel Specificity. *Proc. Natl. Acad. Sci. U.S.A.* **1998**, *95*, 10437−10442.
(10) Clackson, T. Redesigning Small Molecule-Protein Interfaces. *Curr. Opin. Struct. Biol.* **1998**, *8*, 451−458.
(11) Kurumbail, R. G.; Stevens, A. M.; Gierse, J. K.; McDonald, J. J.; Stegeman, R. A.; Pak, J. Y.; Gildehaus, D.; Miyashiro, J. M.; Penning, T. D.; Seibert, K.; Isakson, P. C.; Stallings, W. C. Structural Basis for Selective Inhibition of Cyclooxygenase-2 by Antiinflammatory Agents. *Nature* **1996**, *384*, 644−648.
(12) Gierse, J. K.; McDonald, J. J.; Hauser, S. D.; Rangwala, S. H.; Koboldt, C. M.; Seibert, K. A Single Amino Acid Difference Between Cyclooxygenase-1 (COX-1) and -2 (COX-2) Reverses the Selectivity of COX-2 Specific Inhibitors. *J. Biol. Chem.* **1996**, *271*, 15810−15814.
(13) Clemons, P. A. Design and Discovery of Protein Dimerizers. *Curr. Opin. Chem. Biol.* **1999**, *3*, 112−115.
(14) Spencer, D. M.; Wandless, T. J.; Schreiber, S. L.; Crabtree, G. R. Controlling Signal Transduction with Synthetic Ligands. *Science* **1993**, *262*, 1019−1024.
(15) Amara, J. F.; Clackson, T.; Rivera, V. M.; Guo, T.; Keenan, T.; Natesan, S.; Pollock, R.; Yang, W.; Courage, N. L.; Holt, D. A.; Gilman, M. A Versatile Synthetic Dimerizer for the Regulation of Protein−Protein Interactions. *Proc. Natl. Acad. Sci. U.S.A.* **1997**, *94*, 10618−10623.
(16) Keenan, T.; Yaeger, D. R.; Courage, N. L.; Rollins, C. T.; Pavone, M. E.; Rivera, V. M.; Yang, W.; Guo, T.; Amara, J. F.; Clackson, T.; Gilman, M.; Holt, D. A. Synthesis and Activity of Bivalent FKBP12 Ligands for the Regulated Dimerization of Proteins. *Bioorg. Med. Chem.* **1998**, *6*, 1309−1335.
(17) Holt, D. A.; Luengo, J. I.; Yamashita, D. S.; Oh, H.-J.; Konialian, A. L.; Yen, H.-K.; Rozamus, L. W.; Brandt, M.; Bossard, M. L.; Levy, M. A.; Eggleston, D. S.; Liang, J.; Schultz, L. W.; Stout, T. J.; Clardy, J. Design, Synthesis, and Kinetic Evaluation of High-Affinity FKBP Ligands and the X-ray Crystal Structures of Their Complexes with FKBP12. *J. Am. Chem. Soc.* **1993**, *115*, 9925−9938.
(18) Holt, D. A.; Konialian-Beck, A. L.; Oh, H.-J.; Yen, H.-K.; Rozamus, L. W.; Krog, A. J.; Erhard, K. F.; Ortiz, E.; Levy, M. A.; Brandt, M.; Bossard, M. J.; Luengo, J. I. Structure−Activity Studies of Synthetic FKBP Ligands as Peptidyl-Prolyl Isomerase Inhibitors. *Bioorg. Med. Chem. Lett.* **1994**, *4*, 315−320.
(19) Hatada, M., unpublished results.
(20) Boehm, H.-J.; Klebe, G. What Can We Learn From Molecular Recognition in Protein−Ligand Complexes for the Design of New Drugs? *Angew. Chem., Int. Ed. Engl.* **1996**, *35*, 2588−2614.
(21) Pierce, A. C.; Jorgensen, W. L. Computational Binding Studies of Orthogonal Cyclosporin-Cyclophilin Pairs. *Angew. Chem., Int. Ed. Engl.* **1997**, *36*, 1466−1469.
(22) Redfern, C. H.; Coward, P.; Degtyarev, M. Y.; Lee, E. K.; Kwa, A. T.; Hennighausen, L.; Bujard, H.; Fishman, G. I.; Conklin, B. R. Conditional Expression and Signaling of a Specifically Designed Gi-Coupled Receptor in Transgenic Mice. *Nat. Biotechnol.* **1999**, *17*, 165−169.
(23) Smith, G. K.; Banks, S.; Blumenkopf, T. A.; Cory, M.; Humphreys, J.; Laethem, R. M.; Miller, J.; Moxham, C. P.; Mullin, R.; Ray, P. H.; Walton, L. M.; Wolfe, L. A., III Toward Antibody-Directed Enzyme Prodrug Therapy with the T268G Mutant of Human Carboxypeptidase A1 and Novel In Vivo Stable Prodrugs of Methotrexate. *J. Biol. Chem.* **1997**, *272*, 15804−15816.
(24) Wiederrecht, G.; Hung, S.; Chan, H. K.; Marcy, A.; Martin, M.; Calaycay, J.; Boulton, D.; Sigal, N.; Kincaid, R. L.; Siekierka, J. J. Characterization of High Molecular Weight FK-506 Binding Activities Reveals a Novel FK-506-Binding Protein as Well as a Protein Complex. *J. Biol. Chem.* **1992**, *267*, 21753−21760.
(25) Muhandiram, D. R.; Kay, L. E. Gradient-Enhanced Triple-Resonance Three-Dimensional NMR Experiments with Improved Sensitivity. *J. Magn. Reson., Ser. B* **1994**, *103*, 203−216.
(26) Kay, L. E.; Keifer, P.; Saarinen, T. Pure Absorption Gradient Enhanced Heteronuclear Single Quantum Correlation Spectroscopy with Improved Sensitivity. *J. Am. Chem. Soc.* **1992**, *114*, 10663−10665.
(27) Ikura, M.; Bax, A. Isotope-Filtered 2D NMR of a Protein-Peptide Complex: Study of a Skeletal Muscle Myosin Light Chain Kinase Fragment Bound to Calmodulin. *J. Am. Chem. Soc.* **1992**, *114*, 2433−2440.
(28) Brunger, A. *X-PLOR, Version 3.1. A System for X-ray Crystallography and NMR*; Yale University Press: New Haven, CT, 1992.

JM9904396